

Expulsion Prediction in Resistance Spot Welding

A model is proposed for predicting expulsion in resistance spot welding

BY J. SENKARA, H. ZHANG, AND S. J. HU

ABSTRACT. An expulsion model has been developed for resistance spot welding, based on consideration of the interaction between mechanical and metallurgical processes during welding. An expulsion criterion is proposed by comparing the electrode force with that from the liquid nugget; expulsion occurs when the latter exceeds the former. An effective electrode force, instead of an applied/nominal electrode force, is used in the criterion. This force can be calculated based on the applied electrode force and its offset from the liquid nugget force, which can be obtained through knowledge of the internal pressure and the dimensions of a nugget. Pressure components in a molten metal include those due to melting, liquid expansion, vapor pressure, and decomposition of surface agents, and are formulated by thermodynamic considerations. Experiments have been conducted to verify the model on an aluminum alloy (AA5754), and good agreement was achieved. The model can also be used to develop guidelines for electrode force selection.

Introduction

Expulsion, which can be observed frequently during resistance spot welding, happens at either the faying surface or the electrode/workpiece interfaces. The latter may severely affect surface quality and electrode life, but not the strength of the weld if it is limited to the surface. Therefore, expulsion at the electrode/workpiece interface is not the subject of this work. On the other hand, expulsion at the faying surface is highly undesirable in terms of weld quality because it involves loss of liquid metal from the nugget during welding. The risk of expulsion is especially high in spot welding of aluminum alloys due to the very dynamic and unstable character

of the process, relating to the application of a high current in a short welding time as compared to welding steels. If heavy expulsion occurs, as shown in Fig. 1, a large cavity may form in the nugget after solidification as the result of a deficit in volume, which makes it a serious discontinuity.

However, it is still very common in industrial practice to use high, extreme welding parameters at the border of and sometimes beyond expulsion. This is to meet weld quality requirements for spot weld size, which is widely believed to be the main weld quality indicator. Expulsion is also used as a visual indicator of a "correct" welding process, especially in steel welding, at the expense of introducing discontinuities to weld nuggets. The need to eliminate nonconforming welds in the automotive industry and an increasing trend of using weld-bonding (i.e., resistance spot welding combined with adhesive bonding, in which expulsion may destroy adhesive layers) make it necessary to reduce expulsion in resistance spot welding. Prediction of expulsion is then of important practical interest.

Expulsion in welding involves interactions of mechanical, thermal, and metallurgical processes. For instance, the electric current (together with other welding parameters) determines the heat input rate, which in turn influences the formation of the nugget and the temperature distribution in the weldment. Other factors, such as surface morphology, strength of the workpiece (especially yield strength), loading, and thermal conditions, also influence expulsion. It is difficult to predict or control expulsion; only a few attempts have been made to detect expulsion using various techniques. According to published works, expulsion can be

detected by measuring dynamic resistance (Ref. 1), acoustic emission (Ref. 2), electrode displacement (Refs. 3, 4), and electric signals (Ref. 5). Most of these measurements are difficult to make and often too expensive to use in production. The measurement proposed by Hao et al. (Ref. 5) seemed promising. It described a robust method of monitoring expulsion in aluminum spot welding in high-volume production, based on electric signals for both AC and medium-frequency DC welding machines. All of these efforts are generally for expulsion detection only. Thus, correcting welding parameters to avoid expulsion, if possible at all, can only be done for subsequent welds after making the initial weld. Therefore, the effectiveness of these methods in eliminating expulsion is limited.

A resistance spot welding process, in regard to nugget growth and weld formation, can be divided into several stages. According to Dickinson et al. (Ref. 1), these stages are surface breakdown, asperity softening, temperature rising, formation of molten nugget, nugget growth and mechanical collapse, and expulsion. Similar mechanisms were later introduced by Gould (Ref. 6), who categorized the process into four stages: initiation of nugget, rapid nugget growth, steadily decreasing growth, and expulsion. These stages can be reflected in a typical "lobe" diagram — Fig. 2. Such diagrams, which are widely used in practice to determine welding schedules, only explore the expulsion phenomenon and suggest reasons for expulsion in terms of welding time and welding current. No fundamental understanding can be drawn from them.

Besides experimental study, numerical calculation has also been attempted to investigate expulsion. Browne et al. of Alcan Aluminum Company developed a model for expulsion in spot welding aluminum alloys (Refs. 8–11). In the model, which is the only attempt to date for expulsion prediction, the radius of a molten weld nugget is calculated (by the use of finite element method [FEM]) as a function of time and other parameters. It is assumed in the model that expulsion occurs when the radius of the growing nugget exceeds that of

KEY WORDS

Resistance Spot Welding
Expulsion Prediction
Thermomechanical Analysis
Liquid Nugget
Force Calculation

J. SENKARA is with the Welding Department, Warsaw University of Technology, Warsaw, Poland. H. ZHANG is with the Department of Mechanical, Industrial and Manufacturing Engineering, University of Toledo, Toledo, Ohio, and S. J. HU is with the Department of Mechanical Engineering, University of Michigan, Ann Arbor, Mich.

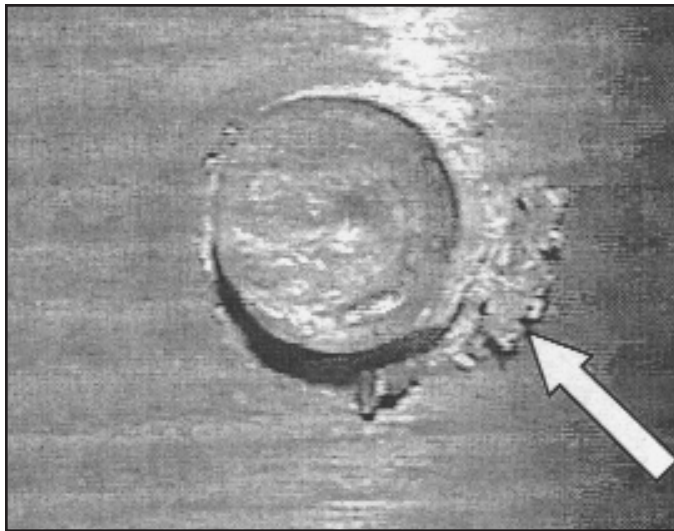


Fig. 1 — A peeled button in aluminum Alloy 5754 with expulsion. The arrow points to a “fan” of ejected and momentarily frozen liquid metal.

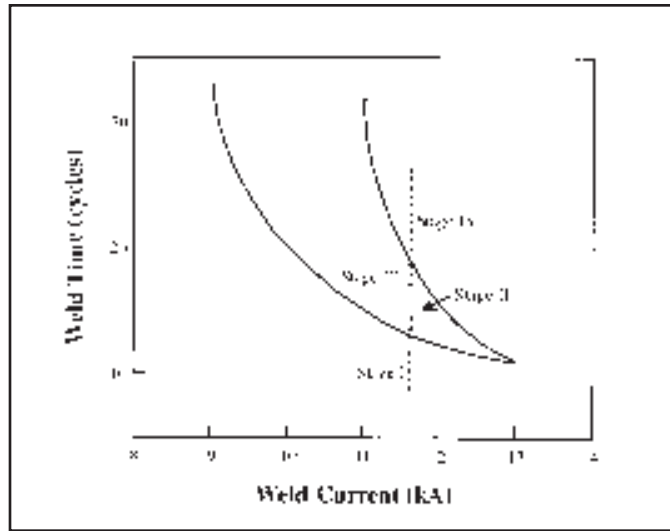


Fig. 2 — Welding stages for a particular current, superimposed on a “lobe” diagram for an HSLA steel, taken from Ref. 7.

the compressive region at the faying interface due to electrode squeezing. The welding condition and process were idealized because of limitations of the numerical model, which relies solely on the comparison of geometric dimensions. Expulsions usually occur at the later stage of welding in this model, as a nugget needs time to grow to a certain size. However, observations have shown that expulsion may also happen at early stages of welding when the size of the molten metal is considerably smaller than that of the compressive force supplied by the electrodes. Expulsion occurs not only from improper welding time, current, or insufficient electrode force, but also from poor electrode and workpiece conditions. In practice, there are rarely cases in which the electrodes are aligned and the fitup is perfect. It has also been recognized that some materials tend to expel more than others. These situations cannot all be covered by the Alcan model.

It is worthwhile to mention the works by Dickinson et al. (Ref. 1) and Wu (Ref. 12). Expulsion takes place, as stated in Ref. 1, when the total useful energy applied to the weld exceeds a certain value defined as “critical expulsion energy,” which is a function of physical properties of the given material. This critical expulsion energy, as well as the total useful energy, is difficult to calculate in practice. Expulsion was related by Wu (Ref. 12) to excessive current densities, either by “gross” peak welding current or by highly localized/microscopic contact areas of faying surfaces with increased resistance from oxidation or contamination, at the early stage of spot welding. Although these studies provided certain insights to the understanding of the expulsion mechanism, they are not applicable for practical use.

In this paper, a new and generic model

of expulsion is presented. The model is developed based on the fundamental physical processes in resistance spot welding, with consideration of the force from the molten metal in the nugget, which is the driving force for expulsion. It is verified by experiments on aluminum Alloy 5754.

A Model for Expulsion Prediction

Principles

Expulsion in welding is determined by many factors involving electrical, thermal, metallurgical, and mechanical processes. Although there are many complicated causes of expulsion, its basic process can be described by the interaction between the forces from the liquid nugget and its surrounding solid containment. Major forces acting on a weldment during welding are illustrated in Fig. 3. They include the squeezing force provided by the electrodes ($F_{E,applied}$) and the force from the liquid nugget (F_N) onto its solid containment, which is generated by the pressure (P) in the molten metal and a compressive force between the workpieces. There is also a resistance to sheet separation provided by solid diffusion (corona bonding) at the faying interface. This force is usually much smaller than the others and can be neglected in the analysis, as this model considers extreme expulsion conditions only.

Based on this understanding, a general model of expulsion is proposed. The criterion can be stated as:

Expulsion occurs when the force from the liquid nugget (F_N) onto the solid containment equals or exceeds the effective electrode force (F_E), i.e., $F_N \geq F_E$.

These forces are shown in Fig. 4. In practice, the applied electrode force is

rarely collinear with the total force from the liquid nugget because of complications in electrode geometry such as wearing, electrode alignment, and part fitup. Therefore, the applied electrode force, in many cases, is not the same as the one used to contain the liquid nugget from expulsion. The “effective” electrode force is introduced in this situation to accurately represent the force used to suppress the force from the liquid nugget.

Evaluation of Effective Electrode Force

An effective electrode force, which is usually a portion of the total applied electrode force, is used to balance the force from the liquid nugget. It can be estimated as follows.

The actual forces on one workpiece can be idealized, as shown by the arrows in Fig. 5, at the time of expulsion. $F_{E,applied}$ is the applied electrode force, F_N is the total force from the liquid nugget against the solid containment, and F_x is a force imposed by the other workpiece. F_E is the effective electrode force, which will be explained in the following.

In Fig. 5, d is the distance between the total nugget force and the electrode force; r is the distance between F_N and the edge of the nugget (it is the radius in the case of a round weld); x is the distance between force F_x and $F_{E,applied}$. Moment equilibrium with respect to the acting point of F_x produces the following relationship between $F_{E,applied}$ and F_N :

$$F_{E,applied}x = F_N(d + x) \quad (1)$$

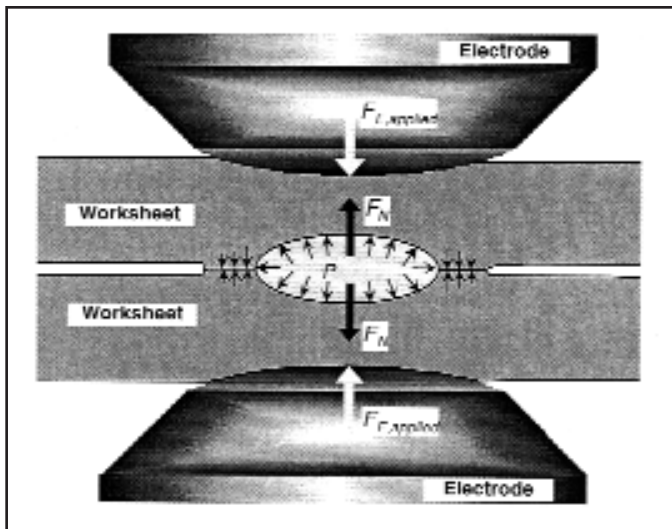


Fig. 3 — Forces acting on the weldment during resistance spot welding in idealized conditions with aligned electrodes and perfect fitup.

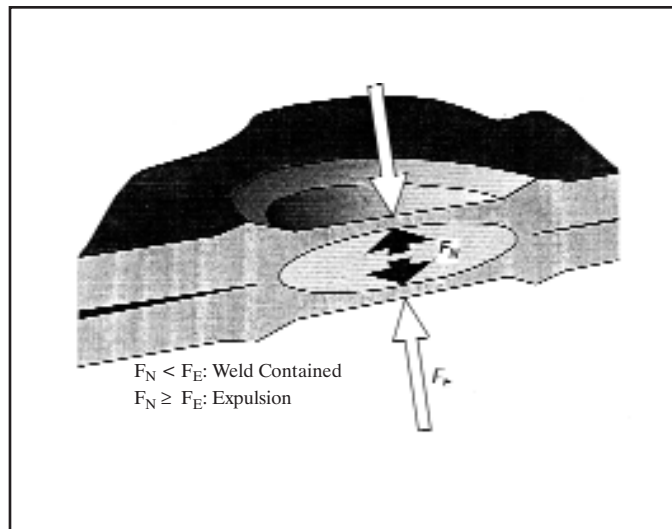


Fig. 4 — Schematic diagram of the balance of forces considered in the model. F_N is the force from the nugget due to liquid pressure and F_E is the effective electrode force.

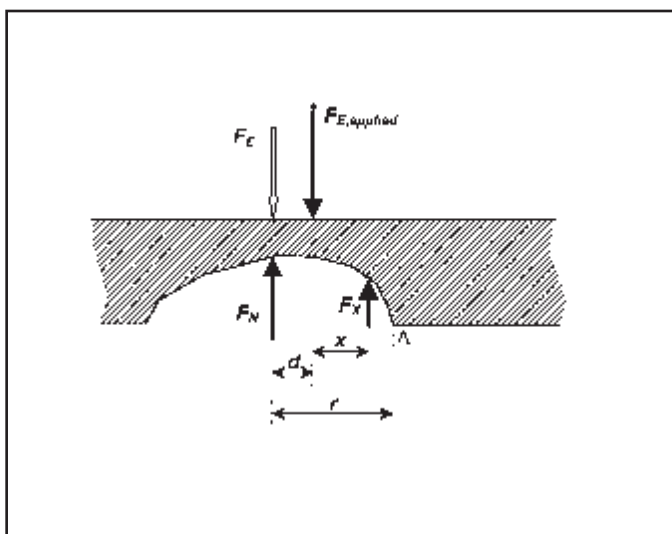


Fig. 5 — Schematic diagram of simplified forces and their locations on one workpiece at expulsion.

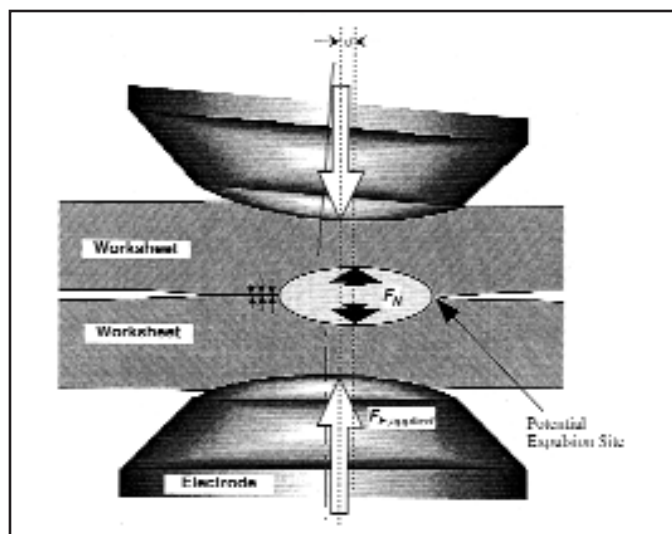


Fig. 6 — An offset between the applied electrode force and that from the nugget, which is created by an angular misalignment of electrodes.

Before metal melts, $x = 0$ because $F_N = 0$, and $F_{E,applied}$ and F_x have to be collinear. As the liquid nugget grows, F_N gets larger ($F_N \propto$ the area of the nugget at the faying surface) so F_x gets smaller because $F_x + F_N = F_{E,applied}$ assuming $F_{E,applied} = \text{constant}$. Meanwhile, x goes up as can be derived from a moment equilibrium with respect to the acting point of $F_{E,applied}$: $F_N d = F_x x$ when assuming $d = \text{constant}$. Because the magnitude of F_N increases and that of F_x goes down, x has to get larger, or F_x gets farther away from the center of the nugget during nugget growth. It is reasonable to assume that when F_x moves across the right edge of the nugget (Point A), the solid loses its containment of the nugget. Therefore, $x = r - d$ can be regarded as a critical condition for expulsion to happen.

Therefore, the expulsion condition is

$$F_{E,applied}(r - d) = F_N r \quad (2)$$

If an equivalent force of a magnitude of

$$F_E = \frac{r - d}{r} F_{E,applied} \quad (3)$$

is applied along the direction of the force from the nugget, the workpiece is under equilibrium. Therefore, when there is a discrepancy between the locations of the electrode force and the force from the nugget, the electrode force can be replaced by an equivalent, or effective, electrode force along the direction of the force from the

nugget. This effective electrode force is smaller than the applied electrode force, i.e., only a portion of the electrode force is used in controlling expulsion. In general, the resultant force imposed by an electrode on a weldment may have both normal and shear components with respect to the workpiece surface. As the shear force does not influence the equilibrium in the direction normal to the sheet, it is not considered in the analysis. Therefore, the applied electrode force refers to the normal component of the total force from an electrode. In most cases, the shear component is expected to be small, and the total force from the electrode can be a good approximation of the applied electrode force.

The discrepancy d is usually created by asymmetric loading, such as in the case of

Table 1 — Selected Properties of Aluminum and Iron, and Main Components in Their Alloys

	Unit	Al	Fe	Cu	Mg	Zn
Solid density at melting point (ρ_S)	10^3 kg m^{-3}	2.55 ^(a)	7.31 ^(a)	8.32 ^(b)	1.65 ^(b)	6.84 ^(b)
Liquid density at melting point (ρ_L)	10^3 kg m^{-3}	2.37 ^(b)	7.07 ^(b)	8.09 ^(b)	1.58 ^(b)	6.64 ^(b)
Liquid density change rate ($-d\rho_L/dT$)	$10^{-1} \text{ kg m}^{-3} \text{ K}^{-1}$	3.11 ^(b)	6.34 ^(b)	9.44 ^(b)	2.60 ^(b)	11.3 ^(b)
Volume change due to melting ($(V_L - V_S)/V_S$)	%	7.06 ^(a)	3.16 ^(a)	4.68 ^(a)	4.2 ^(a)	2.9 ^(a)
Coefficient of volume expansion in liquid at melting point (α)	10^{-4} K^{-1}	1.31 ^(a)	0.89 ^(a)	1.17 ^(a)	1.65 ^(a)	1.70 ^(a)

(a) Calculated values based on data from Refs. 13–16. (b) Data from Ref. 13.

electrode misalignment (axial and angular misalignments), electrode wear, or improper workpiece fitup. It can be approximated by the distance between the geometric center of the indentation marks and that of the nugget. In Fig. 3, the electrodes are aligned and the workpiece fitup is good. The force provided by the electrodes is fully used against the nugget force such that $d = 0$ and $F_E = F_{E,applied}$. However, this aligned and symmetrical system is rarely seen, even in laboratory experiments. Figure 6 shows a case with angular misaligned electrodes. The nugget forms around the shortest electrical current path, which is not the same as where the total electrode force is applied because of the angular misalignment. As a result, an offset d is created between the applied electrode force and the force from the nugget. If insufficient electrode force is applied, expulsion may occur on one side of the nugget, as shown in Fig. 6.

A sectioned nugget of aluminum Alloy

5754 is shown in Fig. 7. The offset is 1.3 mm and, therefore, $F_E \approx 0.7F_{E,applied}$, i.e., only 70% of the applied electrode force was used to suppress expulsion. The location of the applied electrode force is estimated from the surface indentation and the nugget force is at the geometric center of the nugget (its proof will be shown later in this paper).

Electrode force can be applied through pneumatic or other mechanisms and can be approximated, for simplicity, as a constant during welding. The offset is not easy to determine, as it depends on a large number of possibilities of actual welding conditions. A guideline for selecting an electrode force/welding schedule can be obtained by estimating the conditions of extreme cases. The force from the liquid nugget can be calculated with the knowledge of its size and pressure. The following sections are devoted to the calculation of pressures and the resultant force in the molten metal.

Table 2 — Chemical Composition (wt-%) of Commercial Aluminum Alloy 5754 (Ref. 21)

Mg	2.6–3.6
Mn	max. 0.5
Cu	max. 0.1
Fe	max. 0.4
Si	max. 0.4
Ti	max. 0.15
Cr	max. 0.3
Zn	max. 0.2

Pressures and Forces in the Liquid Nugget

The pressure in a liquid nugget is influenced by several factors. As an example, Fig. 8 shows how the volume changes with temperature for pure iron and an Al-Mg alloy. The plots are calculated using specific density data (in solid and liquid states [Refs. 13, 14]) and coefficients of linear thermal expansion (Refs. 15, 16) for Al, Mg, and Fe. During welding, workpieces are heated from an initial temperature to melting point and beyond. A volume increase occurs during heating in the solid state, solid to liquid phase transformation, and heating in the liquid state. The volume change due to melting happens at the melting point for pure metals and between solidus and liquidus temperatures for alloys (except eutectic alloys). This volume change can be significant, as in the case of aluminum (about 7% volume change at its melting point). Further heating of the liquid produces a larger volume increase, which is usually higher than

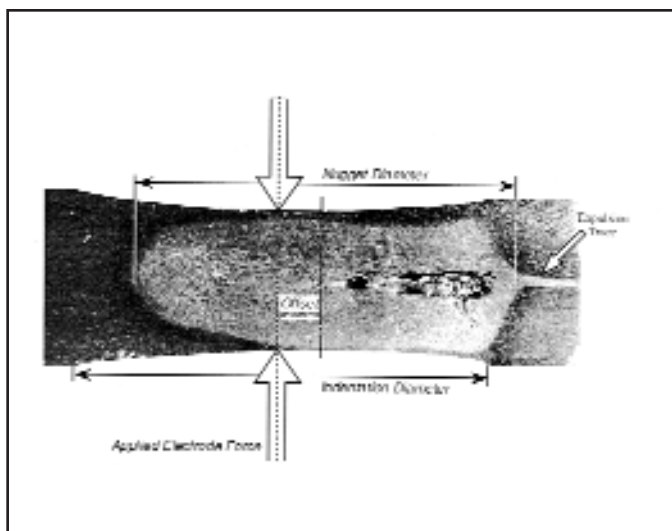


Fig. 7 — A cross section of a nugget in aluminum Alloy 5754 after heavy expulsion. Nugget diameter = 8.93 mm; indentation diameter = 9.94 mm; and offset = 1.30 mm.

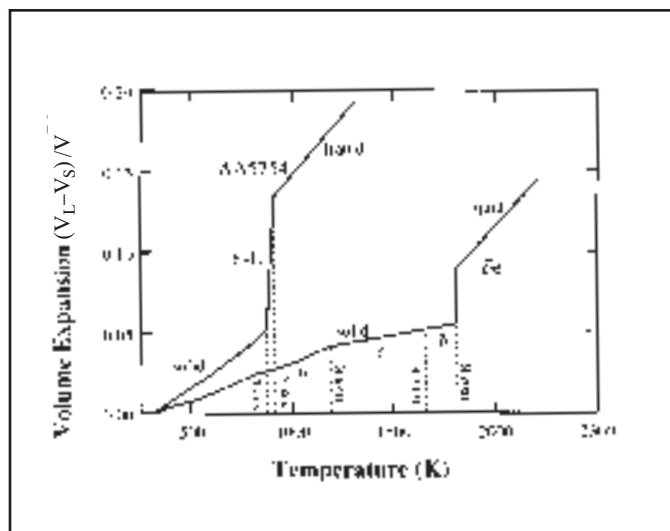


Fig. 8 — Calculated thermal expansion for aluminum Alloy 5754 and pure iron, in the temperature range between room temperature and beyond melting point.

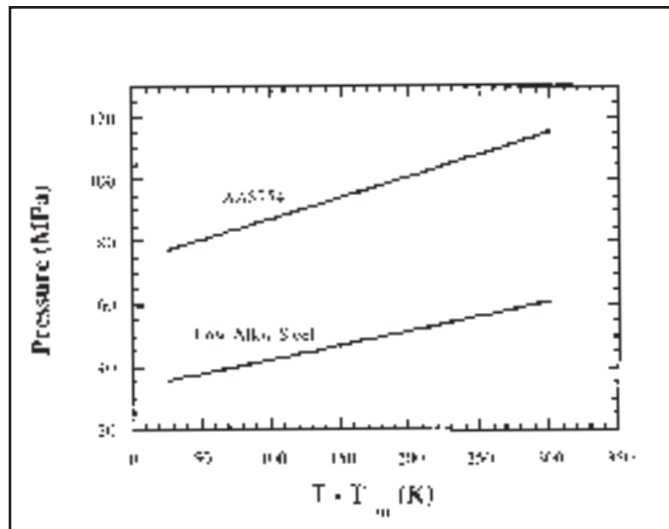
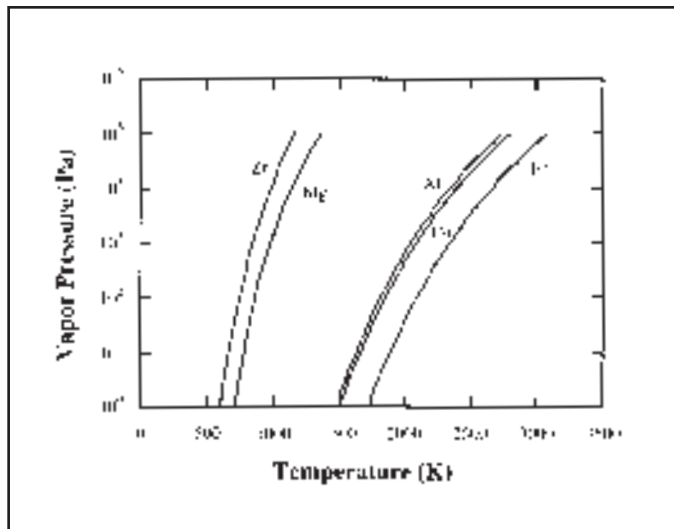


Fig. 9 — Plots of vapor pressures for several metals using data from Ref. 13.

Fig. 10 — Calculated total pressure in liquid nuggets in a low-alloy steel and in aluminum Alloy 5754 as a function of overheating. T_m is the melting temperature.

thermal expansion in the solid state.

However, a free volume expansion of the nugget during resistance spot welding is not possible due to its surrounding solid containment and the squeezing of electrodes. As a result, pressure in the nugget may be significant because of the relatively low compressibility of liquids. It should be noted that if there is expansion of surrounding solids around the liquid nugget, pressure in the nugget will drop. Because the transformation of solid to liquid, which is the major contribution to internal pressure in the nugget, occurs at a relatively narrow temperature range, no significant volume change in the surrounding solid due to thermal expansion is expected. Therefore, for simplicity, the relief of pressure due to simultaneous solid expansion at melting can be neglected. The solids farther away from the molten metal in the workpieces, which have a lower temperature, inhibit the expansion of the solids in the immediate vicinity of the nugget. This confinement, together with the squeezing supplied by the electrodes, makes it difficult for the liquid nugget to expand under the pressure, either from melting or subsequent heating.

Another source of pressure in the liquid nugget is the pressure of metal vapors. Such pressure exists because at temperatures above the melting point, a closed system tends to reach liquid/vapor equilibrium according to general thermodynamic principles. This effect should be taken into account especially if there are volatile elements in the welded alloy, e.g., Mg and Zn in certain series of aluminum alloys or Zn in coated steels. The pressure of metal vapors may be significant even at a temperature below the metal's boiling point. In addition to metal vapor pressure, pressure

from gases resulting from thermal decomposition of surface agents should also be considered. Examples of surface agents are lubricants on metal sheets, pretreatment agents, adhesives (in the case of weld-bonding), and adsorbed moisture or gases. The pressure can be evaluated by considering the type and amount of gaseous products, and their reactivity with, and solubility in, the liquid alloy.

To summarize, there are four major components of pressure in a liquid metal during resistance spot welding: solid to liquid phase transformation (melting), expansion in the liquid state, vapors from the liquid metal, and decomposition of surface agents.

The total pressure in the liquid nugget is the summation of all these components:

$$P = P_{melt} + P_{exp} + P_{vapor} + P_{decomp} \quad (4)$$

In order to calculate the total pressure, the properties of materials above their melting points should be examined. Due to the lack of certain data, an assumption was made so that the properties of an alloy Z_{A-B} of components A and B can be linearly interpolated, using the properties of its components Z_A and Z_B and their atomic fractions x_A and x_B in the alloy:

$$Z_{A-B} = Z_A x_A + Z_B x_B \quad (5)$$

The same assumption is also used for the remaining parts of this paper. The calculation of the four pressure components is detailed below.

Pressure Due to Melting

As the result of melting a certain portion of the metal surrounded by the solid

phase, compression of the liquid takes place. The relationship between the volume V and pressure P in the liquid nugget at a given absolute temperature T can be described by the coefficient of compressibility κ (Ref. 17):

$$\kappa = -\frac{1}{V} \left(\frac{\partial V}{\partial P} \right)_T \quad (6)$$

Therefore, for a small increment of volume, the resulting increase in pressure is

$$dP = \frac{1}{\kappa V} dV \quad (7)$$

Since the molten metal is not allowed to expand freely due to the containment of its solid surrounding and electrode forces, the increase in pressure resulting from melting is approximately the same as that from compressing the liquid metal from V_L to V_S . This pressure can be obtained by integrating Equation 7:

$$\int_0^P dP = - \int_{V_L}^{V_S} \frac{1}{\kappa V} dV \quad (8)$$

where V_S and V_L are molar volumes of solid and liquid states, respectively, at the melting temperature. Therefore, the pressure due to melting is

$$P_{melt} = \int_{V_S}^{V_L} \frac{1}{\kappa V} dV = \frac{1}{\kappa} \ln V \Big|_{V_S}^{V_L} = \frac{1}{\kappa} \ln \frac{V_L}{V_S} \quad (9)$$

So a high volume change during melting results in a high pressure contribution.

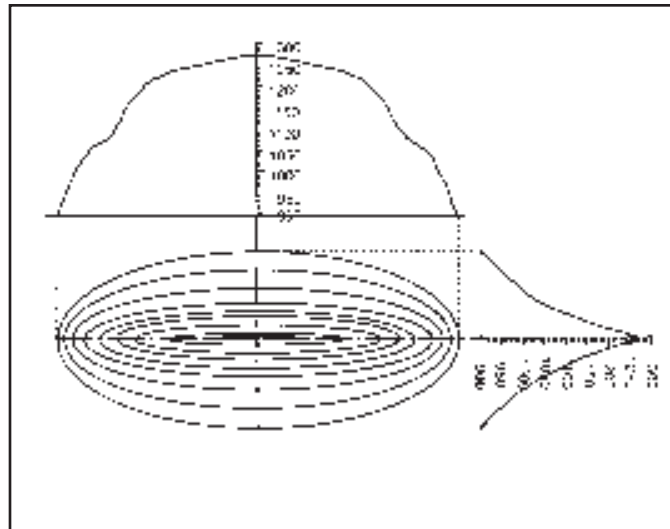
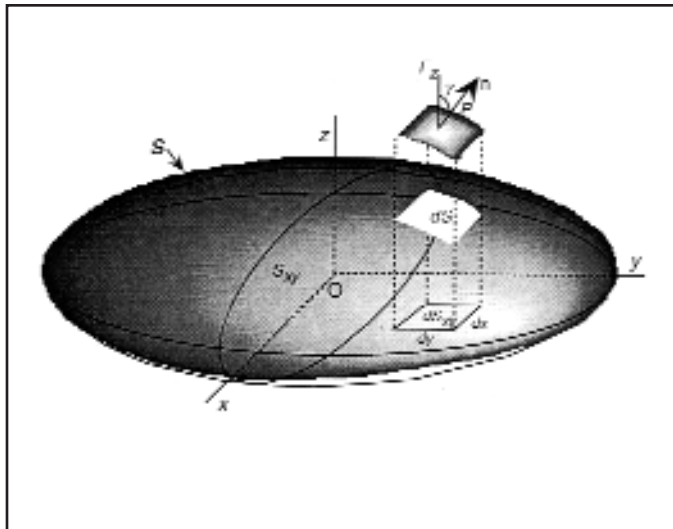


Fig. 11 — Schematic diagram of a liquid nugget. S is the surface (boundary) above the x - y plane. dS is a small segment of S , and dS_{xy} is its projection onto the x - y plane. The total projected area of S is S_{xy} .

Fig. 12 — Temperature distribution predicted by an FEM model (Ref. 20). The elliptical rings are isotherms in the liquid nugget. Temperature is in degrees Kelvin (K).

Volume changes of some metals and alloys are shown in Fig. 8 and Table 1.

Pressure Due to Liquid Expansion

A quantitative relationship between pressure and temperature under a constant volume can be described by thermal pressure coefficient β , defined as (Ref. 17)

$$\beta = \frac{1}{V} \left(\frac{\partial P}{\partial T} \right)_V \quad (10)$$

Its value is unknown for most liquid metals. However, the partial derivative of $\partial P/\partial T$ may be presented as the product of two partial derivatives:

$$\left(\frac{\partial P}{\partial T} \right)_V = - \left(\frac{\partial V}{\partial T} \right)_P \left(\frac{\partial P}{\partial V} \right)_T \quad (11)$$

By introducing a coefficient of volume thermal expansion, α , defined as (Ref. 17)

$$\alpha = \frac{1}{V} \left(\frac{\partial V}{\partial T} \right)_P \quad (12)$$

and using compressibility coefficient κ as defined in Equation 6, β can be expressed by variables whose values can be found in published metallurgical data sources:

$$\beta = \frac{1}{P} \frac{\alpha}{\kappa} \quad (13)$$

Hence, for a small increment of temperature, the increase in pressure is:

$$dP = \frac{\alpha}{\kappa} dT \quad (14)$$

Integration of Equation 14 yields the contribution of pressure due to the expansion of the liquid nugget in the range from melting point T_m to a given temperature T at a constant volume in the following form:

$$P_{exp} = \frac{\alpha}{\kappa} (T - T_{melt}) \quad (15)$$

In Equation 15, κ is a constant, and α can be evaluated by considering the volume change during heating. Because the liquid density depends linearly on the temperature above the melting point, α can be expressed as

$$\alpha = - \frac{C}{\rho_{L,melt} + C(T - T_m)} \quad (16)$$

where $C = -d\rho_L/dT$, a constant that can be derived from the values listed in Table 1. α is listed in Table 1 for several metals.

Vapor Pressure

Vapor pressures of several commonly used metals are presented in Fig. 9. Although pure metals are rarely welded in industrial practice, vapor pressures of alloys can be derived from those of their components.

The total vapor pressure over the liquid alloy, P_{vapor} , equals the sum of partial vapor pressures of particular components \bar{p}_i :

$$P_{vapor} = \sum_i \bar{p}_i \quad (17)$$

According to Raoult's law, \bar{p}_i may be written as a product of thermodynamic activity " a_i " of given component " i " in the liquid solution and its vapor pressure in pure state p_i^0 :

$$\bar{p}_i = a_i p_i^0 \quad (18)$$

where a_i can be written as:

$$a_i = x_i \gamma_i \quad (19)$$

x_i and γ_i are molar ratios of component " i " in the solution and its coefficient of activity, respectively, at a given temperature. Unfortunately, data on a_i and γ_i and their temperature dependence for liquid metallic solutions are limited (Ref. 18), and in many cases, it is impossible to obtain a_i . However, it is possible to calculate γ_i using Gibbs-Duhem's equation of a multicomponent metallic solution:

$$\sum_i x_i d \ln \gamma_i = 0 \quad (20)$$

An especially useful solution of the above equation was developed by Krupkowski (Ref. 19) for quasi-regular metallic solutions. According to his assumption, γ_i is the product of two independent functions of temperature $w(T)$ and concentration $f(x_i)$:

$$\ln \gamma_i = w(T) f(x_i) \quad (21)$$

In two-component solutions (A-B), co-

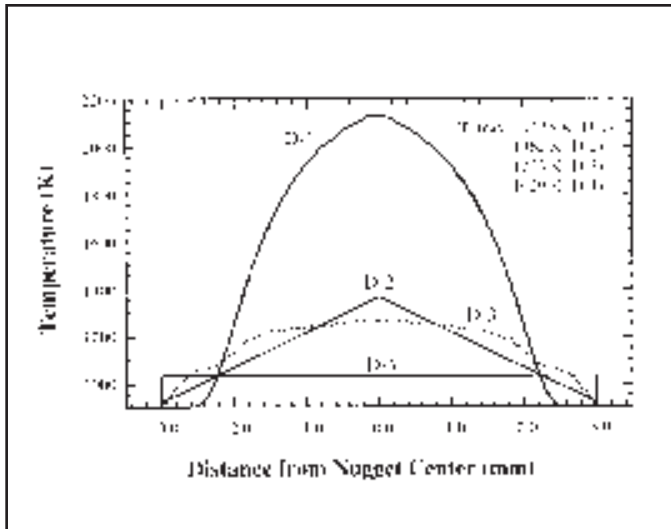


Fig. 13 — Temperature distributions in a nugget. The dashed line (D-3) is taken from an FEM simulation (Ref. 20), and the solid lines are three assumed temperature distributions.

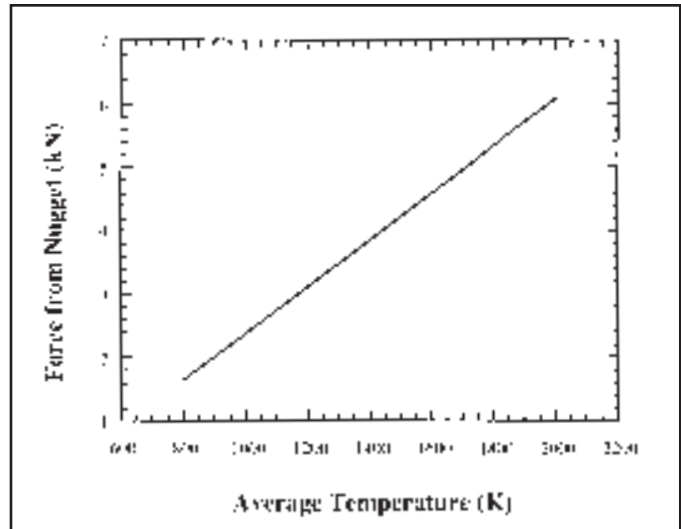


Fig. 14 — Nugget force vs. average temperature in the nugget. The properties of a pure Al nugget of 6 mm diameter are used.

efficients of activity can be expressed as

$$\ln \gamma_A = \left(\frac{a}{T} + b \right) x_B^m \quad (22)$$

and

$$\ln \gamma_B = \left(\frac{a}{T} + b \right) \left(x_B^m - \frac{m}{m-1} x_B^{m-1} + \frac{1}{m-1} \right) \quad (23)$$

where a , b , and m are constants that can be found in thermodynamic tables or calculated from existing data. Based on two-component solutions, the calculation of γ_i in a multicomponent solution is also possible by using the following equation:

$$\ln \gamma_i = \sum_{j=1, k=2}^{j=n-1, k=n} [\ln \gamma_i]_{j,k} \quad (24)$$

where $[\ln \gamma_i]_{j,k}$ is for the activity coefficient of i in a binary j - k solution.

Pressure Due to Decomposition of Surface Agents

Before spot welding, there are usually lubricants, adhesives, and other coatings on the faying interfaces. Additionally, thin layers of adsorbed gases and moisture may also exist on the surfaces. During spot welding, the heat releases gases and decomposes surface agents at the faying interfaces. A part of the gases is trapped by rapidly spreading liquid metal at the faying surface under electrode forces. Examples of such gases are H_2 , H_2O , CO , CO_2 , and C_xH_y chains. The type and amount of gases may vary in individual cases. However, the general steps of calculation of their contributions to the total nugget

pressure are as follows:

- Determine the types of particular gases in the weld area and calculate the quantities (in terms of moles) under the standard condition (at 298 K).
- Subtract the amount of gases dissolved in or reacted with the liquid metal. Gas/metal solubility as a function of temperature, as well as chemical affinity, should be considered.
- Calculate the pressure increase at the welding temperature (above T_m) with the knowledge of the total pressure contributed by other factors.

In practice, the amount of specific gases released from the sheet surface may be determined by suitable chemical analysis. Thorough decomposition and zero gas solubility and reactivity can be assumed to obtain extreme values of pressure due to surface agents.

The calculation of pressure from surface agent decomposition depends on the particular gas composition, solubility, and reactivity of the system. By using the ideal gas equation of state for the released gases, an equation for the pressure can be derived by thermodynamic considerations as

$$\kappa P_{decomp} + \ln \left(V_{nugget} - \frac{nRT}{P_{decomp} + P_L} \right) - \ln V_{nugget} = 0 \quad (25)$$

In Equation 25, $n = n_{total} - n_{diss.} - n_{react.}$, where n_{total} is the sum of the moles of the released gases under standard thermodynamic conditions, and $n_{diss.}$ and $n_{react.}$ are the moles of gases dissolved in and reacted with the liquid metal at the welding tem-

perature (T), respectively; R is the universal gas constant, and V_{nugget} is the volume of the liquid nugget; and P_L is the total pressure due to melting, liquid expansion, and metal vapor pressure. Equation 25 can be solved numerically for particular systems.

Total Pressure and Force from Liquid Nugget

The total force from the nugget can be estimated numerically (e.g., by using the finite element method). The liquid nugget can be considered as a simply connected domain. The minimum temperature is at the solid/liquid boundary, which is the melting temperature (solidus can be used for simplicity). Finite element simulation (Ref. 20) shows that the maximum temperature is reached at the center of the nugget, and isotherms in the nugget are ellipsoidal in shape. Therefore, the temperature distribution in the liquid nugget can be approximated as layers (or shells), with the temperature being constant in each layer/shell. For any shell i reaching the melting point in the liquid nugget, the total pressure is

$$p_i = p_{i1} + p_{i2} + p_{i3} + p_{i4} \quad (26)$$

where partial pressures p_{i1-3} are as expressed in Equations 9, 15, and 17, and p_{i4} is the partial pressure due to the decomposition of surface agents that can be calculated from Equation 25. Total pressure in the entire nugget is

$$P = \frac{1}{V_{nugget}} \int_{V_{nugget}} p dV \approx \frac{1}{V_{nugget}} \sum_i p_i V_i = \sum_i p_i f_i \quad (27)$$

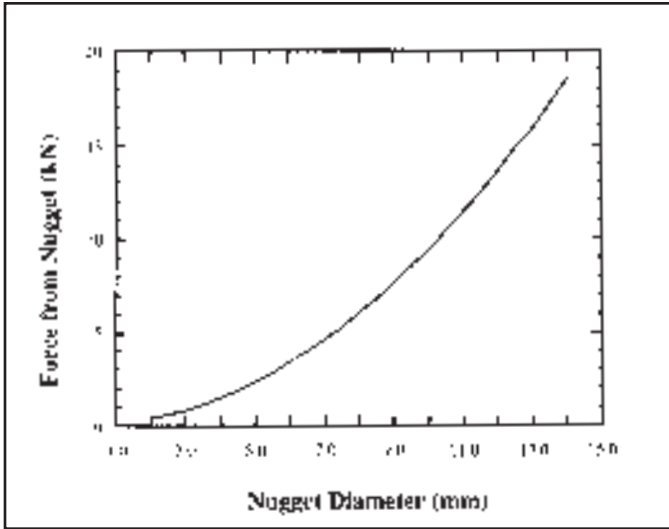


Fig. 15 — Dependency of nugget force on weld diameter for Al. An average temperature of 1275 K is assumed in the nugget.

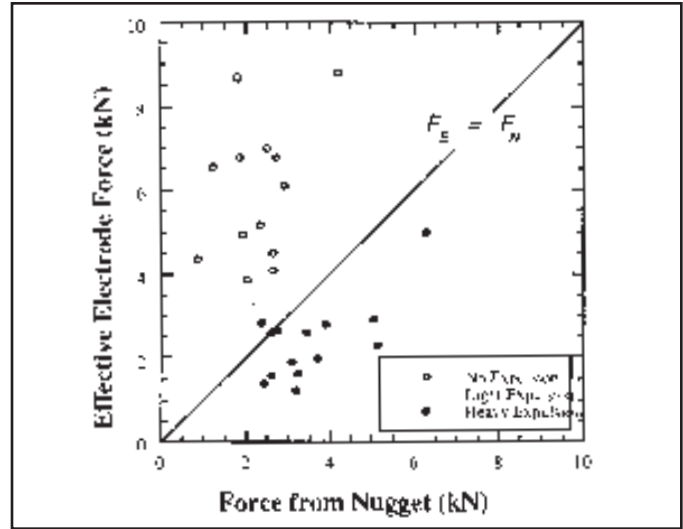


Fig. 16 — Comparison of model prediction and experimental observation.

where p is the total pressure of a unit volume at a temperature, V_i is the volume of shell i in which the temperature is assumed constant, and f_i is the volume fraction of shell i . A detailed calculation of pressures is demonstrated in the following sections. Figure 10 shows examples of calculated total pressures.

Force from the liquid nugget onto its solid surroundings can be estimated once the pressure and the projected area in the direction of concern are known. Force in the direction of interest (here it is assumed to be the z -direction) on a segment of solid/liquid interface dS (as shown in Fig. 11) is

$$dF_z = PdS \cos\gamma = PdS_{xy} \quad (28)$$

where γ is the angle between the z -axis and the normal n of dS ; and dS_{xy} is the projection of dS onto the x - y plane. The total force in z -direction is

$$F_z = \int_S dF_z = P \int_S dS_{xy} = PS_{xy} \quad (29)$$

where S_{xy} is the projection area of the nugget on the x - y plane. Therefore, the total force is independent of particular shapes of nuggets. It also implies that the center of the total force is the geometric center of S_{xy} .

Calculation of Pressures and Forces

The expulsion model proposed in this paper is a general one. It does not distinguish the source of forces or materials. Therefore, it can be used in spot welding of

steels as well as aluminum alloys. Aluminum alloys are more sensitive to expulsion than steels, and the effect of electrode force is more significant, because of aluminum's higher electrical and thermal conductivity, lower melting point, and higher thermal expansion (both in solid and liquid state), as well as other properties. In this section, the calculation of forces from the liquid nugget, as well as use of the expulsion model, are demonstrated for the aluminum Alloy 5754. The chemical composition of Alloy 5754 is listed in Table 2.

Force from the liquid nugget can be calculated with the knowledge of the pressure inside the nugget and the size of the nugget. Among the four major pressure components, i.e., pressure due to solid-to-liquid transformation, liquid expansion, liquid vapor pressure, and surface agents, are all dependent on temperature, except pressure due to melting. Therefore, it is important to know the temperature distribution in the liquid nugget. Once the temperature for a particular volume of liquid is known, the total pressure can be calculated by knowing the major component elements and using the equations obtained

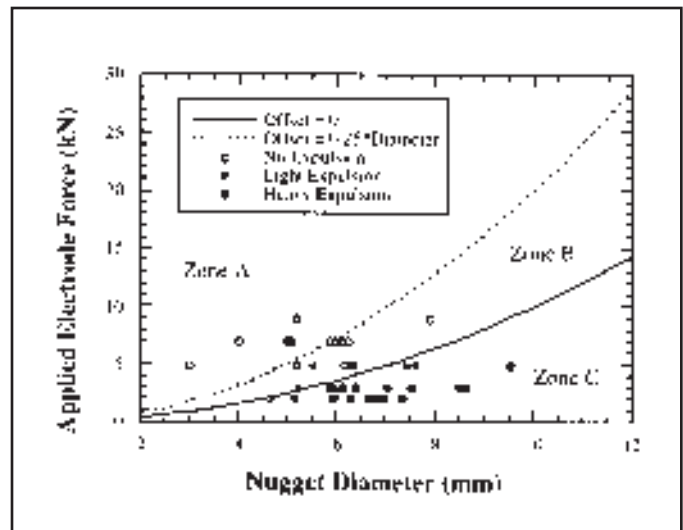


Fig. 17 — Estimated electrode force to suppress expulsion in aluminum Alloy 5754. Solid dots and circles are data from the experiment, as shown in Fig. 16.

in the previous section. In general, the procedure for calculating the pressure and force from a liquid nugget can be outlined in the following:

- Obtain material properties of the main alloying elements and surface contaminants.
- Obtain information of temperature distribution and value, and dimensions of the nugget.
- Calculate pressure components and the total pressure.
- Calculate forces in the directions of interest.

Temperature in the molten metal during welding is commonly conceived as nonuniform, as shown in Ref. 6. Conversely, Alcini (Ref. 22) claimed that tem-

perature is uniform throughout the molten nugget. To obtain some knowledge about possible temperature distributions in the nugget, results of a finite element simulation (Ref. 20) are shown in Fig. 12. Isotherms are approximated by ellipsoidal surfaces (or ellipses for two-dimensional cases). This is a nugget formed after 160 ms of welding for Alloy 5754 with a welding current (medium-frequency direct current) of 28 kA and an electrode force of 7 kN. Temperature gradients are different along the width and height directions. Pressure components calculated based on the temperature distribution predicted by the finite element simulation results are

$$\begin{aligned} P_{melt} &= 74.05 \text{ MPa} \\ P_{exp} &= 18.49 \text{ MPa} \\ P_{vapor} &= 0.01 \text{ MPa} \end{aligned}$$

and the ratio of pressures is

$$P_{melt} : P_{exp} : P_{vapor} \approx 80:20:0 (\%)$$

The pressure component due to surface agents was not calculated because their quantities were not determined in this case.

The calculated force in the height direction is 2.62 kN. Because the contributions of vapor and surface agents to the total pressure are usually small, they can be neglected in estimating liquid pressure and force from the nugget. Therefore, from Equations 26 and 27, the total pressure can be expressed as

$$P = \frac{1}{V_{nugget}} \int_{nugget} p dv = \frac{1}{V_{nugget}} \int_{nugget} P_{melt} dv + \frac{1}{V_{nugget}} \int_{nugget} P_{exp} dv \quad (30)$$

By substituting Equations 9 and 15 for P_{melt} and P_{exp} , Equation 30 can be rewritten as

$$P = \frac{1}{\kappa} \ln \frac{V_L}{V_S} + \frac{\alpha}{\kappa} (T_{avg} - T_{melt}) \quad (31)$$

where

$$T_{avg} = \frac{1}{V_{nugget}} \int_{nugget} T dv$$

is the average temperature in the nugget.

Assuming a liquid nugget of ellipsoidal shape with axes a , b ($= a$), and c (in the thickness direction), T_{avg} can be approximated as

$$T_{avg} = \frac{1}{V_{nugget}} \int_{nugget} T dv = \frac{3}{a^3} \int_0^a Tr^2 dr \quad (32)$$

where r is the distance from the nugget center along one axis (a). Equation 31 shows that the total pressure will be the same for two different temperature distributions if they have the same average temperatures. It can be seen from Equation 32 that the influence of local temperature on the average temperature is not uniform. A shell far from the nugget center has more volume, and therefore, more "weight" on the average temperature, than a shell close to the nugget center if these two shells have the same thickness. Because of the quadratic term " r^2 " in Equation 32, an average temperature of a nugget cannot be calculated by averaging the area under the curves of distribution, such as those shown in Fig. 13. This figure shows four arbitrary temperature distributions in nuggets of the same dimensions calculated from the same amount of heat input. The resultant average temperature (1029 K) is the same for all four types of distributions. Because T_{avg} is the same, the total pressure in the liquid nugget is the same, as is the force from the nugget with the same geometric dimensions. Therefore, a detailed temperature distribution is not of importance for force calculation. Figure 14 shows the dependence of force on average temperature in a nugget of 6 mm diameter. There is approximately a 0.5 kN force increase for every 100 K rise in temperature.

The dependency of force from the nugget on the nugget size is shown in Fig. 15. A fixed average temperature of 1275 K is used for all nugget sizes. If the electrode force and the force from the nugget are not aligned, an effective electrode force, which is a fraction of the applied electrode force, must be large enough to balance the force from the nugget to avoid expulsion.

Experimental Verification of the Expulsion Model

To verify the expulsion model, experiments were conducted on aluminum Alloy 5754. This alloy is being used on a limited scale as structural material in the automobile industry. The sheets were supplied by Alcan and treated by an Alcan surface treatment technique to ensure a repeatable surface condition. A scissors gun with a medium-frequency direct-current (MFDC) transformer was used in the experiments. The welding parameters were chosen to cover a wide range of possibilities. Electrode force was in the range of 2 to 9 kN, electrical current was between 20 and 35 kA, and welding time was varied between 67 ms (4 cycles) and 167 ms (10 cycles).

During welding, the occurrence of expulsion was monitored, and its severity was classified as light or heavy, depending

on the magnitude of sudden changes in electrode displacement monitored during the experiment. Welded samples were then cut, ground, polished, and etched using standard metallographic techniques. The nugget diameter, size of electrode indentation, and offsets between the nugget center and indentation center were measured by microscopy. The dimensions measured are shown in Fig. 7. Based on the results of the finite element model, shown in the previous section, the average temperature for each weld when it was in a liquid state was estimated. An assumption was made that the average temperature in the liquid nugget was proportional to the total heat input after deducting the heat necessary to melt the nugget. This approximation avoids all thermal-electrical details during the welding process. However, the possible error caused by this assumption is small, as the contribution of pressure due to liquid expansion is usually less than 20% of the total pressure, as shown in the previous section. The force from a liquid nugget can then be calculated, using the weld dimensions and the average temperature, by the procedure outlined in the previous section. Equation 3 was used to calculate the effective electrode force.

The results of calculated force from the nugget vs. effective electrode force are plotted in Fig. 16. The diagonal line represents the equilibrium boundary between the two forces, and expulsion is expected when a point falls on or below this line according to the model. As shown in the figure, most expulsion points are below the boundary and some are around the vicinity of the line, although a few points with expulsion are above the diagonal. There are a few possible reasons for this discrepancy. First, it is not always easy to accurately measure the nugget size and offset. This is related mostly to the asymmetric nugget growth in some cases due to electrode misalignment and electrode wear. Other random factors in welding may also influence the measurement. Another possible source of error is the limitation of this model, which uses the applied electrode force and ignores detailed pressure distribution imposed by the electrodes onto the workpieces. Including such a consideration may improve the accuracy of the model. In spite of these factors, the model's predictions fit well with the experiments in general, proving that it is important to distinguish the effective electrode force from the nominal electrode force.

Prospective Application

Because expulsion is highly undesirable, it is important not only to detect, but

to predict and control its occurrence in welding practice. The proposed model can serve such purposes.

First, the model provides a guideline for the selection of electrode force. Figure 17 shows the levels of electrode force needed to suppress expulsion, with the uncertainty of welding conditions taken into account. An average temperature of 1275 K in the liquid nugget is assumed for Alloy 5754. If the system is perfect, i.e., the electrodes are aligned and the fitup is good, the offset between the applied electrode force and the force from the nugget is zero. The expulsion/no expulsion boundary is shown by the solid line and is the minimum electrode force needed to contain the nugget. This kind of ideal welding condition rarely exists, and the degree of nonconformity varies dramatically in practice. If an offset of a quarter of the nugget width is assumed, the applied electrode force to contain the same nuggets is twice their minimum values, as shown by the dashed line in Fig. 17. Assuming this is the worst case, then if the electrode force is chosen in Zone A, the probability of expulsion is low. In Zone C, the risk of expulsion is high. Whether it happens in Zone B depends on the welding condition. In experiments conducted to verify the model, offsets of $0.01\text{--}0.38 \times$ nugget width have been observed. The same set of data was also plotted in Fig. 17. There is no expulsion for the data points falling in Zone A, and expulsion for all in Zone C. All possibilities (no expulsion, light expulsion, and heavy expulsion) are observed in Zone B. The experimental results have basically confirmed the model prediction. In addition to expulsion, other factors, such as the influence of the electrode force on electrode indentation and contact resistance, should also be considered when choosing an electrode force.

Second, it is possible to use this model to control expulsion. The use of this model requires the knowledge of 1) the applied electrode force, 2) the force from the liquid nugget, and 3) the offset. The model provides a detailed procedure for the calculation of the nugget force based on thermodynamic and mechanical analyses. Variables of the model can be easily calculated and no complicated algorithms are involved. These advantages provide an opportunity for this model to be used in an actual welding environment to predict and, furthermore, control expulsion.

It is important to know the material properties, especially those at elevated temperatures, in the application of the model. Some of them are not available but can be approximated by using the knowledge of those in existing databases, as demonstrated in previous sections. Because the model is based on fundamental

mechanical and thermodynamic analyses, it is applicable not only to particular materials or processes, but also for various materials and systems.

Summary

A systematic methodology is proposed to analyze forces involved in resistance spot welding. These forces are used to develop a criterion of expulsion. In summary:

- A generic model was proposed for expulsion prediction based on the interaction of forces acting on a weldment during resistance spot welding.
- A detailed and systematic procedure was proposed to evaluate the pressure in the liquid nugget by thermodynamic analysis.
- The force from the liquid nugget was derived from the pressure and the size of the nugget.
- The effective electrode force was calculated by knowing the offset between the applied electrode force and the force from the nugget.
- The model was verified by experiments on an aluminum alloy.

A quantitative knowledge of the evolution of nuggets in shape and location is the basis for accurate prediction of expulsion, on which more research is needed.

Although the model was verified by experiments on an aluminum alloy, it should not be considered as a model for expulsion prediction in aluminum welding only. It is equally applicable to other material systems.

Acknowledgments

The authors are grateful for the help provided by Douglas R. Boomer, Innoval Technology Ltd., and for the financial support of this work by the Advanced Technology Program (ATP/NIST) through the Intelligent Resistance Welding Consortium.

References

1. Dickinson, D. W., Franklin, J. E., and Stanya, A. 1980. Characterization of spot welding behavior by dynamic electrical parameter monitoring. *Welding Journal* 59(6): 170-s to 176-s.
2. Vahaviolos, S. J., Carlos, M. F., and Slykhouse, S. J. 1981. Adaptive spot-weld feedback control loop via acoustic emission. *Materials Evaluation* 39(10): 1057–1060.
3. Kilian, M., and Hutchenreuther, A. 1994. Monitoring and control of electrode indentation. *Proc. AWS Sheet Metal Welding Conference VI*. Detroit, Mich. Paper No. C4.
4. Hao, M., Osman, K. A., Boomer, D. R., and Newton, C. J. 1996. Developments in characterization of resistance spot welding of aluminum. *Welding Journal* 75(1): 1-s to 6-s.
5. Hao, M., Osman, K. A., Boomer, D. R., Newton, C. J., and Sheasby, P. G. 1996. On-line

nugget expulsion detection for aluminum spot welding and weld bonding. *SAE Paper No. 960172*.

6. Gould, J. 1987. An examination of nugget development during spot welding using both experimental and analytical techniques. *Welding Journal* 66(1): 1-s to 10-s.

7. Han, Z., Indacochea, J. E., Chen, C. H., and Bhat, S. 1993. Weld nugget development and integrity in resistance spot welding of high-strength cold-rolled sheet steels. *Welding Journal* 72(5): 209-s to 216-s.

8. Newton, C., Browne, D. J., Thornton, M. C., Boomer, D. R., and Keay, B. F. 1994. The fundamentals of resistance spot welding aluminum. *Proc. AWS Sheet Metal Welding Conference VI*. Detroit, Mich. Paper No. E2.

9. Browne, D. J., Chandler, H. W., Evans, J. T., and Wen, J. 1995. Computer simulation of resistance spot welding in aluminum — part I. *Welding Journal* 74(10): 339-s to 344-s.

10. Browne, D. J., Chandler, H. W., Evans, J. T., James, P. S., Wen, J., and Newton, C. J. 1995. Computer simulation of resistance spot welding in aluminum — part II. *Welding Journal* 74(12): 417-s to 422-s.

11. Browne, D. J., Newton, C., and Boomer, D. R. 1995. Optimization and validation of a model to predict the spot weldability parameter lobes for aluminum automotive body sheet. *Proc. International Body Engineering Conference IBEC'95—Advanced Technologies & Processes* pp. 100–106.

12. Wu, K. C. 1977. The mechanism of expulsion in weld bonding of anodized aluminum. *Welding Journal* 56(8): 238-s to 244-s.

13. Lide, D. R., ed. 1993–1994. *Handbook of Chemistry and Physics*. 74th Ed. CRC Press.

14. ASM. 1977. *Metals Handbook*. Vol. 1, 8th Ed. Metals Park, Ohio.

15. ASM. 1983. *ASM Metals Reference Book*. 2nd Ed. Metals Park, Ohio.

16. Hatch, J. E., ed. 1984. *Aluminum: Properties and Physical Metallurgy*. Metals Park, Ohio: ASM.

17. Prigogine, I., and Defay, R. 1967. *Chemical Thermodynamics*. London, U.K.: Longmans.

18. Hultgren, R., Orr, R. L., Anderson, P. D., and Kelley, K. K. 1974. *Selected Values of Thermodynamic Properties of Metals and Alloys*. J. Wiley.

19. Krupkowski, A. 1974. *Basic Problems in Theory of Metallurgical Processes*. Warsaw: Polish Scientific Publishing (in Polish).

20. Zhang, H., Huang, Y., and Hu, S. J. 1996. Nugget growth in spot welding of steel and aluminum. *Proc. AWS Sheet Metal Welding Conference VII*. Detroit, Mich. Paper No. B3.

21. Alcan Rolled Products Company. *Automotive Sheet Specification*. 1994.

22. Alcini, W. V. 1990. Experimental measurement of liquid nugget heat convection in spot welding. *Welding Journal* 69(5): 177-s to 180-s.

**HOTTEST WELDING
BOOKS ON THE WEB**

www.aws.org/catalogs